

RESEARCH REPORT

The simultaneous interaction of MSL2 with CLAMP and DNA provides redundancy in the initiation of dosage compensation in *Drosophila* males

Evgeniya Tikhonova¹, Anna Fedotova¹, Artem Bonchuk¹, Vladic Mogila¹, Erica N. Larschan², Pavel Georgiev^{1,*} and Oksana Maksimenko^{1,*}

ABSTRACT

The binding of the *Drosophila* male-specific lethal dosage compensation complex (DCC) exclusively to the male X chromosome provides an excellent model system to understand mechanisms of selective recruitment of protein complexes to chromatin. Previous studies showed that the male-specific organizer of the complex, MSL2, and the ubiquitous DNA-binding protein CLAMP are key players in the specificity of X chromosome binding. The CXC domain of MSL2 binds to genomic sites of DCC recruitment *in vitro*. Another conserved domain of MSL2, named Clamp-binding domain (CBD) directly interacts with the N-terminal zinc-finger domain of CLAMP. Here, we found that inactivation of CBD or CXC individually only modestly affected recruitment of the DCC to the X chromosome in males. However, combination of these two genetic lesions within the same MSL2 mutant resulted in an increased loss of DCC recruitment to the X chromosome. Thus, proper MSL2 positioning requires an interaction with either CLAMP or DNA to initiate dosage compensation in *Drosophila* males.

KEY WORDS: MSL, CLAMP, Sex determination, Transcription factor, C2H2 zinc finger, CXC

INTRODUCTION

In *Drosophila* males, a multisubunit dosage compensation complex (DCC) is responsible for a precise compensatory increase in the expression of genes on the X chromosome (Kuroda et al., 2016; Lucchesi, 2018; Samata and Akhtar, 2018). The DCC consists of five proteins, MSL1, MSL2, MSL3, MOF and MLE, and includes two redundant non-coding RNAs, *roX1* (3.7 kb) and *roX2* (0.6 kb) that perform similar functions (Lucchesi, 2018; Samata and Akhtar, 2018). MSL2 is expressed only in males and is the core DCC component, suggesting a key role in binding specificity of DCC to the X chromosome (Kuroda et al., 2016). The interaction between MSL1 and MSL2 proteins forms the structural core of the DCC, and the C-terminal PEHE domain of MSL1 is responsible for interactions with MSL3 and MOF (Li et al., 2005; Kadlec et al., 2011; Hallacli et al., 2012). The MLE protein, an ATP-dependent RNA/DNA helicase of the DEAD subfamily, interacts with two

noncoding roX RNAs, *roX1* and *roX2*, to induce their unwinding (Maenner et al., 2013; Ilik et al., 2017), which allows them to bind to MSL2. Thus, roX RNAs link MLE and MSL2 proteins into a single complex.

One of the key questions is what is responsible for the specificity of DCC binding to the X chromosome of males. An incomplete DCC containing only MSL1 and MSL2 binds to an invariant set of about 200 sites on the X chromosome, which are called the primary chromatin entry sites (CES) (Alekseyenko et al., 2008) or high-affinity sites (HAS) (Straub et al., 2008). Structural analysis showed that the CXC domain of MSL2 specifically recognizes a GA-rich sequence motif within the HAS/CES (Fauth et al., 2010; Zheng et al., 2014).

Using *in vitro* genome-wide DNA-binding assays, it was demonstrated (Villa et al., 2016) that MSL2 alone specifically binds to a subclass of HAS/CES named PionX (pioneering sites on the X). A zinc-finger protein called CLAMP (Chromatin Linked Adaptor for MSL Proteins) was found to be important for binding of the DCC on the X chromosome (Larschan et al., 2012; Soruco et al., 2013). CLAMP is an essential protein in *Drosophila* that is expressed in both sexes and binds thousands of GA-rich sequences across the genome (Soruco et al., 2013; Kuzu et al., 2016; Urban et al., 2017a). CLAMP directly interacts with MSL2 and opens chromatin at HAS, which promotes DCC recruitment (Urban et al., 2017a; Albig et al., 2019).

Here, we examined the role of the CXC and CLAMP-binding domains of MSL2 in recruiting the DCC to the X chromosome. We show that these two domains have overlapping and partially redundant functions in ensuring proper positioning of the DCC on the X chromosomes in *Drosophila* males, thus permitting its proper function.

RESULTS AND DISCUSSION

Mutations and deletions of CXC and CLAMP-binding domain (CBD) do not affect the stability of MSL2 mutants

The MSL2 protein is crucial for recruitment of DCC to the X chromosome in males (Lyman et al., 1997; Straub et al., 2013). The main aim of this work was to assess the roles of the CLAMP-binding domain (CBD) and CXC in the ability of MSL2 to recruit DCC to the X chromosome (Fig. 1A, Fig. S1).

In a previous study (Albig et al., 2019), CBD was mapped within the 620–685 aa region of MSL2. In order to make highly precise mutations in MSL2, we have refined the interacting regions within the MSL2 and CLAMP proteins using a glutathione S-transferase (GST) pulldown assay *in vitro* (Fig. 1B). We tagged the 573–708 aa region of MSL2 and the 1–196 aa region of CLAMP with either GST or Thioredoxin-6xHis-tag. The GST protein and the 6xHis-tagged MSL2 RING domain (1–196 aa) were used as negative

¹Department of the Control of Genetic Processes, Institute of Gene Biology, Russian Academy of Sciences, 34/5 Vavilov Street, Moscow 119334, Russia. ²Department of Molecular Biology, Cell Biology, and Biochemistry, Brown University, Providence, Rhode Island 02912, USA.

*Authors for correspondence (georgiev_p@mail.ru; maksog@mail.ru)

© A.B., 0000-0002-0948-0640; V.M., 0000-0003-2398-0331; P.G., 0000-0002-6509-3194; O.M., 0000-0003-3502-0303

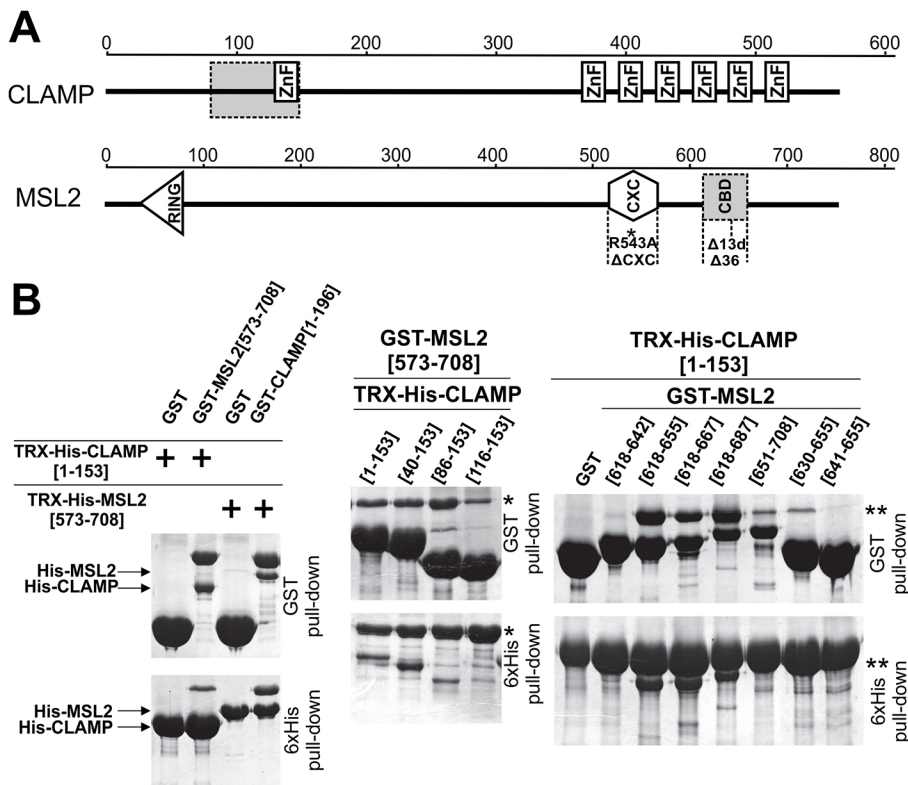


Fig. 1. Mapping CBD in MSL2 and transgenic lines expressing MSL2 mutations. (A) Schematic of full-length CLAMP and MSL2 proteins. The scale shows the number of amino acid residues. Boxes with dashed lines indicate regions involved in interaction between MSL2 and CLAMP. Dashed lines indicate deletions in full-size MSL2 protein that were used in this work. ZnF, zinc-finger domain. (B) Mapping of interacting domains of CLAMP and MSL2 proteins in *in vitro* pull-down assays. The positions of amino acids are given in square brackets. Asterisk marks position of GST-MSL2[573-708]. Two asterisks mark position of Thioredoxin-6xHis-CLAMP[1-153].

controls. Both GST- and 6xHis-tag pull-down assays confirmed interaction between 1-196 aa of CLAMP and 573-708 aa of MSL2. To refine the interacting domains further, we developed a set of deletion derivatives of the GST-tagged MSL2 and Thioredoxin-6xHis-tagged CLAMP. The pull-down experiments showed that a region between aa 86 and 153 of CLAMP containing the zinc-finger and the preceding 30 aa interact with MSL2. It was also found that 618-655 aa of MSL2 are crucial for its interaction with CLAMP. It turned out that the CLAMP-interacting region in MSL2 is highly conserved within the *Drosophila* family, similar to the RING and CXC domains (Fig. S1).

To characterize the domains of MSL2 that contribute to the recruitment of DCC to the X chromosome, we expressed in flies different cDNA variants of MSL2, tagged with 3×FLAG (Fig. 1A). To better define CBD, we made a deletion not only of the whole 620-655 aa region (MSL2^{Δ36}), but also of the distal 642-654 aa (MSL2^{Δ13d}) part. To ablate activity of the CXC domain, we used a previously characterized point mutation in this domain (Li et al., 2008; Villa et al., 2016) that substitutes the arginine at position 543, which is essential for DNA binding, by alanine [R543A (R*)]. We also made constructs expressing the MSL2^{ΔCXC} mutant lacking the CXC domain, and the MSL2^{R*Δ13d} mutant, which combines R* and Δ13d.

A strong ubiquitin (Ubi) promoter was used to express cDNAs encoding these MSL2 variants. Overexpression of MSL2 under this Ubi promoter allowed problems associated with low stability MSL2 mutant variants to be overcome. All transgenes were inserted at the same 86Fb region on the 3rd chromosome, using a φC31-based integration system (Bischof et al., 2007). Immunoblot analysis showed that all MSL2 variants were present in the transgenic flies at nearly equivalent levels (Fig. S2). The relative stability of MSL2 variants makes it possible to compare their ability to recruit DCC on the X chromosome.

CXC and CBD functions are partly redundant in the ability of MSL2 to recruit DCC to the X chromosome in males

To test role of CXC and CBD in specific recruitment of the DCC in males, we introduced transgenes into the null *msl2*^{γ227} background (Zhou et al., 1995). Unexpectedly, all the single-mutant variants of MSL2 (MSL2^{Δ36}, MSL2^{Δ13d}, MSL2^{ΔCXC} and MSL2^{R*}) were able to complement the *msl2*^{γ227} null mutation and considerably restored viability in males homozygous for the null mutation (Fig. 2A). Only *msl2*^{γ227} null males carrying the MSL2^{R*Δ13d} transgene showed very low viability, and early mortality (5-7 days after eclosion). Thus, dosage compensation is strongly compromised in the MSL2^{R*Δ13d} mutant, which lacks the ability to bind to both CLAMP and DNA.

Next, we tested binding of DCC to the polytene chromosomes in males carrying different variants of the MSL2 protein (Fig. 2B, Figs S3, S4). In all cases, binding of MSL1 was correlated with the binding of the MSL2 variants. In male MSL2^{Δ13d}, MSL2^{R*} or MSL2^{ΔCXC} larvae, we observed reduced binding of MSL2-FLAG and MSL1 to the X chromosome (Fig. S4). The binding of MSL1 and MSL2-FLAG was much more strongly diminished in MSL2^{R*Δ13d} males. Additional MSL1/MSL2 bands were found on the polytene autosomes in all tested transgenic lines (Fig. 2B, Fig. S4) suggesting that MSL complexes started to bind to the lower-affinity sites on autosomes.

To compare binding of MSL complex in different mutants, we selected previously characterized representative binding sites for MSL complex: PionX sites (Villa et al., 2016), CES sites (Aleksyenko et al., 2008), and several sites on the autosomes that have MSL2 signal (Straub et al., 2013). We found that MSL2-FLAG and MSL1 bound to all PionX and CES sites in males expressing wild-type MSL2 (Fig. 2C). The MSL2^{R*} and MSL2^{Δ13d} had the same binding patterns at all tested sites, with no difference between PionX and CES (Fig. 2C, Fig. S5): at 12 sites, binding of MSL1 and

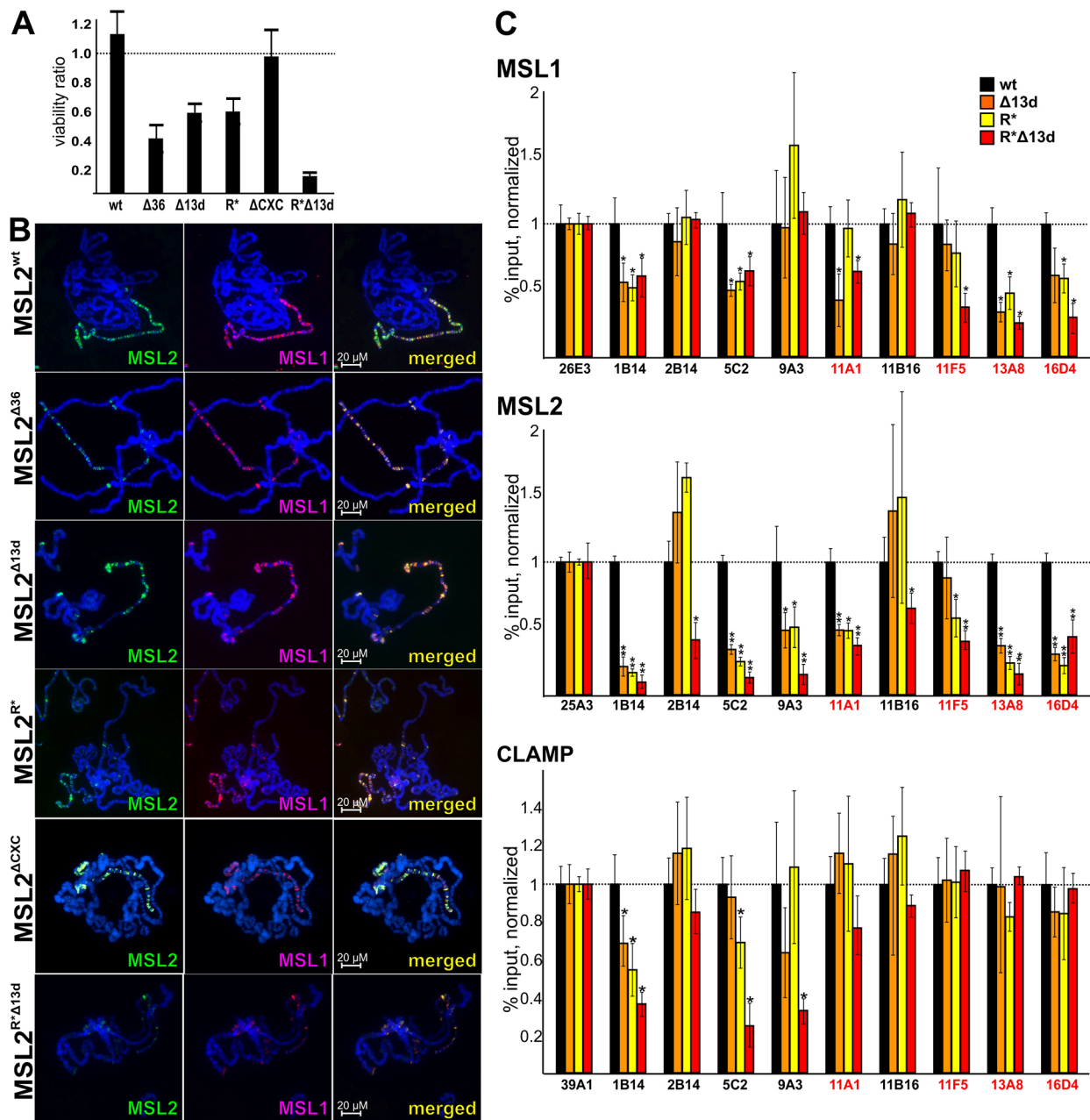


Fig. 2. Testing functional activity of MSL2 mutants in males. (A) Viability (as a relative percentage) of male adult flies after expression of MSL2 derivatives on the *msl2^{γ227/msl2^{γ227}}* (*msl2*-null) background. Flies expressing corresponding MSL2 derivatives in heterozygous *msl2^{γ227}/CyO* flies were used as internal controls with 100% viability. Results are expressed as mean±s.d. of three independent crosses. (B) MSL1 and MSL2 localization on the polytene chromosomes from 3rd day male larvae on the *msl2*-null background expressing different FLAG-tagged variants of MSL2 protein. Panels show immunostaining of 3×FLAG-MSL2 protein with mouse anti-FLAG antibody (green) and MSL1 protein with corresponding rabbit antibody (magenta). DNA was stained with DAPI (blue). (C) Comparison of binding of MSL1, MSL2 and CLAMP at different CES and PionX (marked with red text) regions in the MSL2-expressing flies on the *msl2^{γ227}* background. Histograms show ChIP enrichments at the CES regions on chromatin isolated from male flies expressing different MSL2 variants: MSL2^{wt} (wt), MSL2 ^{$\Delta 13d$} ($\Delta 13d$), MSL2^{R*} (R*), MSL2^{R* $\Delta 13d$} (R* $\Delta 13d$). The results are presented as a percentage of input genomic DNA normalized to corresponding positive autosomal genomic regions for MSL1 (26E3) and MSL2 (25A3), and compared with binding levels in the flies expressing wild-type MSL2 protein (corresponding to the '1' on the scale). Error bars show s.d. of quadruplicate PCR measurements for three independent experiments. **P*<0.05, ***P*<0.01.

the MSL2 mutant proteins was reduced nearly 50%; at three sites (2B14, 11B16, and 13D4) binding of both proteins did not change in mutant larvae. The point mutation R543A (R*) in the CXC domain and its complete deletion (ΔCXC) displayed similar patterns of MSL1/MSL2/CLAMP binding to the selected sites (Fig. S6).

Similar to the results obtained with polytene chromosomes, the MSL2^{R* $\Delta 13d$} double mutant, which ablates interaction with both CLAMP and DNA, showed diminished chromatin

immunoprecipitation (ChIP) enrichment compared with MSL2^{R*} or MSL2 ^{$\Delta 13d$} single mutants at most locations (Fig. 2C). At the 16D4 site, both single and double MSL2 mutants had similar significant reductions in binding. In two cases, 2B14 and 11B16, only the binding of MSL2^{R* $\Delta 13d$} was reduced. Binding of MSL1 only partially correlated with recruitment of MSL2 variants to the same sites. This might be explained by the ability of MSL1 to be recruited as a component of alternative complexes. In most cases,

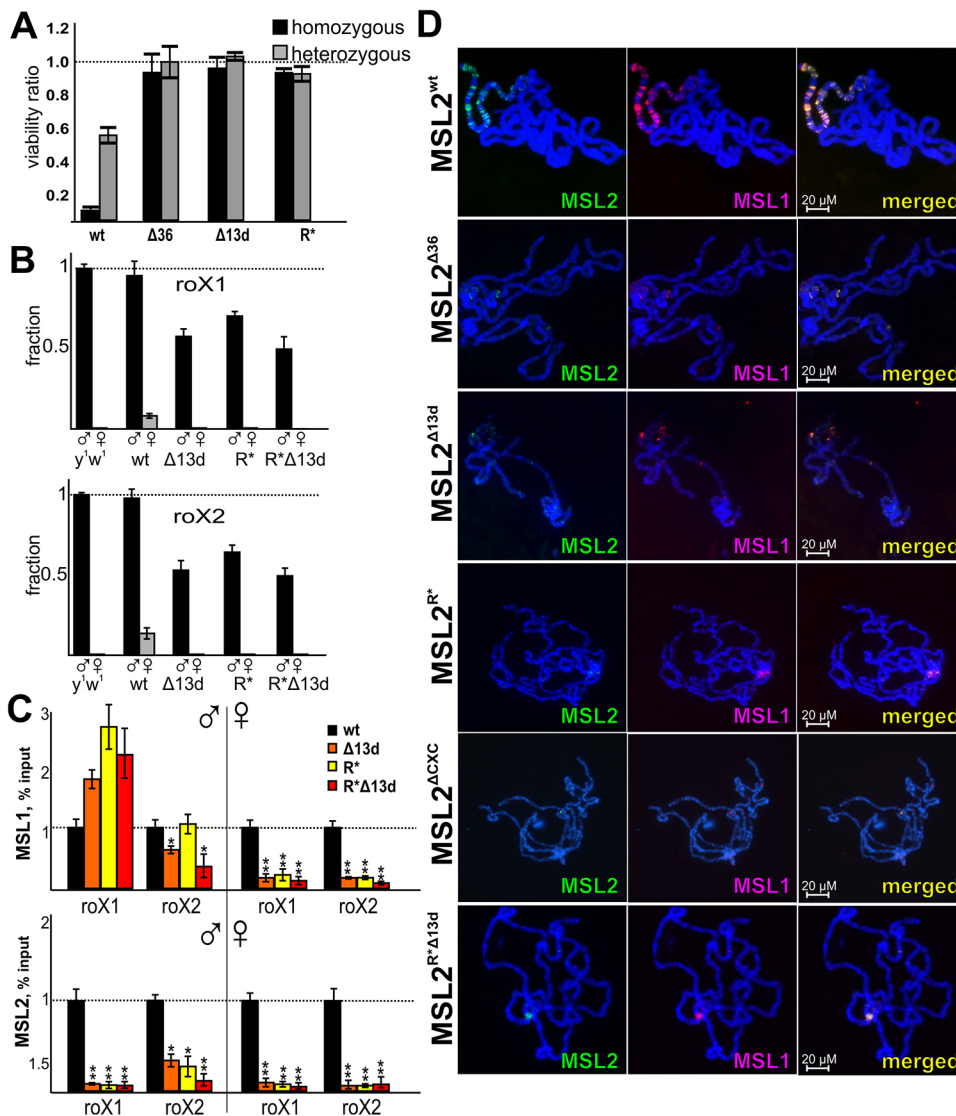


Fig. 3. Testing functional activity of MSL2 mutants in females. (A) Viability (as a relative percentage) of females to male adult flies after expression of MSL2 derivatives (wt, Δ13d, R*, R*Δ13d). Results are expressed as mean±s.d. of three independent crosses in homozygous (black) and heterozygous (gray) lines. (B) Expression levels of the *roX1* and *roX2* RNAs in male and female larvae in the *y¹w¹* flies (wild-type background) and MSL2-expressing flies (wt, Δ13d, R*, R*Δ13d) on the *msl2^{y227}* background. Individual transcript levels were determined by RT-qPCR with corresponding primers normalized relative to *Rpl32* for the amount of input cDNA. Histogram shows the changes of mRNAs for the tested roX genes compared with expression levels in wild-type flies (*y¹w¹*, '1' on the scale). Error bars show s.d. ($n=3$). (C) Comparison of binding of MSL1 and MSL2 in the *roX1* and *roX2* CES regions in the MSL2-expressing flies on the *msl2^{y227}* background. (D) Distribution of the MSL complex on the polytene chromosomes from 3rd day female larvae expressing different FLAG-tagged variants of MSL2 protein. Other designations are as in Fig. 2.

CLAMP binding did not change in lines expressing different MSL2 variants (Fig. 2C). However, strong reduction of the CLAMP binding was observed at the 1B14, 5C2 and 9A3 sites in males expressing MSL2^{R*Δ13d}. Thus, in some cases, CLAMP binding depends on recruitment of the DCC, correlating with the synergy observed between MSL2 and CLAMP occupancy (Sorucu et al., 2013; Albig et al., 2019).

Interestingly, at some autosomal sites, binding of MSL1 (in MSL2^{R*} and MSL2^{Δ13d} flies), but not the MSL2 mutant proteins, was reduced (Fig. S7). This result suggests an existence of alternative mechanisms of MSL2 recruitment to sites outside of the DCC.

CXC and CBD cooperate in recruiting DCC to the X chromosome in females

Ectopic expression of MSL2 in females resulted in assembly of a functional DCC (Kelley et al., 1997) that led to a strong elevation of gene expression and, as a consequence, a decrease in viability. As expected, females carrying homozygous MSL2^{wt} transgenes had low viability (Fig. 3A). In contrast, we observed normal viability in females carrying homozygous transgenes expressing mutant versions of MSL2 affecting either CXC or CBD. These results

suggest that functional activity of these transgenic MSL2 variants was at least partially compromised.

In wild-type female larvae, the *roX* RNAs are not expressed (Meller et al., 1997). Expression of wild-type MSL2 in females resulted in a significant activation of the *roX2* RNA and, to a lesser extent, the *roX1* RNA (Rattner and Meller, 2004). We confirmed that the expression of MSL2 in females induced transcription of both *roX* RNAs (Fig. 3B). However, expression of the *roX* RNAs in females was lower than in corresponding males, as expected. The *roX* RNAs were also not expressed in females expressing mutant versions of MSL2 with mutations in either CXC or CBD, or both.

The HAS/CES located near the *roX* genes are required for stimulation of their transcription in males and repression in females (Bai et al., 2004; Urban et al., 2017b). We performed ChIP to determine whether MSL2 mutants are normally recruited to the known HAS/CES adjacent to the *roX* genes (Fig. 3C). ChIP showed that MSL2 and MSL1 were bound to these HAS/CES in the MSL2^{wt} transgenic female larvae. In contrast, the MSL2 mutants in which the CXC domain was disrupted or contained deletions of the CBD failed to recruit MSL2 or MSL1. These results demonstrate a direct correlation between the binding of MSL1/MSL2 and the activation of the *roX* genes in females.

Polytene chromosomes in the females are a useful model system to define protein domains that are essential for recruiting the DCC to the X chromosome (Zhou et al., 1995; Li et al., 2008; Morra et al., 2011). Transgenic expression of MSL2 in females led to localization to the X chromosomes of both the MSL2 and MSL1 proteins, confirming that MSL2 expressed under the Ubi promoter is able to recruit DCC to the X chromosome in females (Fig. 3D). Inactivation of the CXC domain in the MSL2^{R*} or MSL2^{ΔCXC} transgenic larvae led to binding of either mutant to several sites on different chromosomes and to the centromeric region (Fig. 3D, Fig. S8). MSL1 was colocalized at the same sites, suggesting that MSL2 lacking a functional CXC domain redirects recruitment of MSL complex to new sites. Deletions in CBD (MSL2^{Δ36}, MSL2^{Δ13d} and MSL2^{R*Δ13d}) resulted in an almost complete absence of binding sites for the mutant variants of MSL2 and MSL1. These results suggest that CXC and CBD function cooperatively to recruit DCC onto the X chromosome.

A model of specific recruitment of the DCC to the HAS/CES

MSL2 was previously suggested as a key protein in recruitment of the DCC to the X chromosome (Lyman et al., 1997; Li et al., 2008; Villa et al., 2016). Unexpectedly, deletion of the CXC domain and the R543A point substitution showed similar weak effects on the recruitment of the DCC in males. This result is in accordance with a previous observation that mutations of two cysteines, forming architecture of the CXC domain, did not significantly reduce male survival (Lyman et al., 1997). At the same time, mutant MSL2 lacking both activities (DNA binding and interaction with CLAMP) failed to rescue the null *msl2*^{γ227} mutant in males effectively. Thus, the MSL2-CLAMP interaction and recognition of DNA by the CXC domain cooperatively contribute to the specificity of DCC recruitment to CES/HAS *in vivo*.

The phenotype of MSL2^{R*Δ13d} flies includes poor male survival and decreased targeting of DCC to the X chromosome, similar to that observed in flies lacking both roX genes (Meller and Rattner, 2002). It seems likely that an important role in the initial recruitment of the DCC to the HAS/CES is played by MLE, which binds to the core MSL complex through the roX RNAs (Li et al., 2008; Straub et al., 2013; Quinn et al., 2014). The CXC and CLAMP-binding domains are essential for the initial recruitment of the MSL sub-complex (which likely also includes MSL1, MSL3 and MOF) to the regulatory regions of the roX genes. For this reason, specific binding of MSL sub-complex (MSL1/MSL2) has become completely dependent on the CXC and CBD in females. In males, roX gene expression is less dependent on binding of the MSL complex (Meller et al., 1997; Bai et al., 2004). This might be a likely explanation for why inactivating the CXC or CBD only partially reduced recruitment of the DCC to the X chromosomes in males, but is fully required in females.

Importantly, even the double MSL2 mutant can partially support recruitment of the DCC to the X chromosome. The mutant MSL2^{R*Δ13d} still organized DCC by forming the core complex with MSL1 through the RING domain and recruiting MLE via roX RNA. Previously, the N-terminal domain (84 aa) of MSL1 was shown to be required for recognition of the X chromosome by the DCC (Scott et al., 2000; Li et al., 2005). To explain functional redundancy of MSL2 domains in males, we propose a model in which multiple protein-protein and CXC-DNA interactions are responsible for the specificity of DCC recruitment to the male X chromosome (Fig. 4). In the future, identification of additional proteins that directly interact with the components of DCC, will be key to understanding the mechanisms of selective recruitment of the DCC to HAS/CES on the X chromosome.

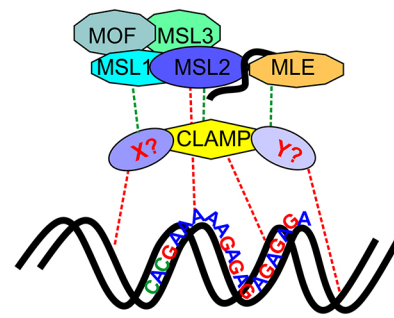


Fig. 4. Model explaining redundancy and cooperativity of CBD and CXC in functional activity of MSL2. Red dashed lines show potential DNA-protein contacts, green dashed lines show protein-protein interactions.

MATERIALS AND METHODS

Plasmid construction

For *in vitro* experiments, protein fragments were either PCR-amplified using corresponding primers, or digested from MSL2 or CLAMP cDNA and subcloned into pGEX-4T1 (GE Healthcare) or into a vector derived from pACYC and pET28a(+) (Novagen) bearing p15A replication origin, Kanamycin resistance gene, and pET28a(+) MCS.

To express 3×FLAG-tagged MSL2 and 3×HA-tagged CLAMP in the S2 cells, protein-coding sequences were cloned in frame with 3×FLAG and 3×HA, excised, and subcloned into the pAc5.1 plasmid (Life Technologies). Plasmids for the yeast two-hybrid assay were prepared using the full-sized and truncated versions with separate domains of MSL2 and CLAMP as C-termini fused with pGBT9 and pGAD424 vectors from Clontech. PCR-directed mutagenesis was used to make constructs with mutated MSL2 (corresponding primers are given in Table S1). Different full-sized variants of MSL2 were fused with 3×FLAG at the C terminus and cloned into an expression vector. This vector contains an *attB* site for φC31-mediated recombination, the *Ubi67c* promoter with its 5'UTR, a 3'UTR with SV40 polyadenylation signal, and the intronless *yellow* gene as a reporter for detection of transformants. Details of the cloning procedures, primers, and plasmids used for plasmid construction are available in Table S2.

Pulldown assays

BL21 cells co-transformed with plasmids expressing GST-tagged and 6×His-tagged derivatives of MSL2 and CLAMP were grown in LB media to an A600 of 1.0 at 37°C and then induced with 1 mM IPTG at 18°C overnight. ZnCl₂ was added to final concentration 100 μM before induction. Cells were disrupted by sonication, centrifuged at 13,000 *g* for 30 min, applied to resin for 10 min at 4°C, followed by four washes with buffer C (see below) containing 500 mM NaCl. GST pulldown was performed with Immobilized Glutathione Agarose (Pierce) in buffer C [20 mM HEPES-KOH, pH 7.7, 150 mM NaCl, 10 mM MgCl₂, 0.1 mM ZnCl₂, 0.1% NP40 and 10% (w/w) glycerol]. The bound proteins were eluted with 50 mM reduced glutathione, 100 mM Tris-HCl, pH 8.0, 100 mM NaCl for 15 min. The 6×His-pulldown was performed similarly, with Zn-IDA resin (Cube Biotech) in buffer A (50 mM HEPES-KOH, pH 7.6, with 500 mM NaCl, 5 mM MgCl₂, 0.1 mM ZnCl₂, 20 mM imidazole, 5% glycerol, 0.1% NP-40 and 5 mM β-mercaptoethanol) containing 1 mM PMSF and Calbiochem Complete Protease Inhibitor Cocktail VII (5 μl/ml), washed with buffer A containing 30 mM imidazole, and proteins were eluted with buffer B (50 mM HEPES-KOH, pH 7.6, with 500 mM NaCl, 250 mM imidazole and 5 mM β-mercaptoethanol), 20 min at +4°C.

Antibodies

Antibodies against MSL1 (aa 423-1030), MSL2 (aa 421-540), CLAMP (aa 222-350) were raised in rabbits and purified from the sera by ammonium sulfate fractionation followed by affinity purification on CNBr-activated Sepharose (GE Healthcare) or Aminolink Resin (Thermo Fisher Scientific) according to standard protocols. Affinity-purified antibodies were tested with immunoblot analysis (Fig. S9). Mouse monoclonal anti-FLAG (clone

M2, F1804, 1:500) and anti-HA (clone HA-7, H3663, 1:200) antibodies were from Sigma-Aldrich.

Cell culture, transfection

Drosophila S2 cells were grown in SFX medium (HyClone) at 25°C. Transfection of plasmids was performed with the Cellfectin II reagent (Invitrogen) according to the manufacturer's instructions. Typically, cells were transfected in six-well plates and grown for 24–48 h before harvesting.

Co-immunoprecipitation assay

S2 cells grown in SFX medium were co-transfected by 3×FLAG-MSL2 (with deletions) and 3×HA-CLAMP plasmids with Cellfectin II (Life Technologies), as recommended by the manufacturer. After transfection, the cells were incubated for 48 h and then collected by centrifugation at 700 g for 5 min, washed once with 1×PBS and re-suspended in 20 packed cell volumes of hypotonic lysis buffer (20 mM Tris-HCl, pH 7.4, with 10 mM KCl, 10 mM MgCl₂, 2 mM EDTA, 10% glycerol, 1% Triton X-100, 1 mM DTT and Calbiochem Complete Protease Inhibitor Cocktail V). After incubation on ice for 10 min, the cells were sonicated (2×15 s on ice at 20% output, 40% duty cycle), NaCl was added to a final concentration of 420 mM, and incubation on ice continued for 60 min, with periodic mixing. Sonication was repeated as above to reduce viscosity, cell debris was pelleted by centrifugation at 10,000 g for 30 min at 4°C, and the supernatant was collected for immunoprecipitation with anti-CLAMP antibodies, incubated with Protein A Agarose (Pierce), and equilibrated with incubation buffer-150 (20 mM Tris-HCl, pH 7.4, 150 mM NaCl, 10 mM MgCl₂, 1 mM EDTA, 1 mM EGTA, 10% glycerol and 0.1% NP-40). Rabbit IgG conjugated to Protein A Agarose beads (by incubating in the same buffer on a rotary shaker at 4°C for 1 h) were used as negative control. The protein extract (50 µg protein) was adjusted to a volume of 500 µl with buffer-150, mixed with antibody-conjugated beads (30 µl), and incubated on a rotary shaker overnight at 4°C. The beads were then washed with one portion of incubation buffer-500 (buffer-150 with 500 mM NaCl), one portion of incubation buffer-300 (buffer-150 with 300 mM NaCl), and one portion of incubation buffer-150, re-suspended in SDS-PAGE loading buffer, boiled, and analyzed by western blotting. Proteins were detected using the ECL Plus Western Blotting substrate (Pierce) with anti-FLAG (clone M2, F1804, Sigma-Aldrich, 1:500) and anti-HA (clone HA-7, H3663, Sigma-Aldrich, 1:200) antibodies.

Fly crosses and transgenic lines

Drosophila strains were grown at 25°C under standard culture conditions. The transgenic constructs were injected into preblastoderm embryos using the ϕC31-mediated site-specific integration system at locus 86Fb (Bischof et al., 2007). The emerging adults were crossed with the *yac^{w1118}* flies, and the progeny carrying the transgene in the 86Fb region were identified by *y⁺* pigmented cuticle.

Viability (as a relative percentage) of *msl2^{γ227}/msl2^{γ227}* males expressing different MSL2 derivatives (MSL2*) was calculated as a ratio of males to females in *msl2^{γ227}/msl2^{γ227}*; MSL2*/MSL2* lines. Viability (as a relative percentage) of females expressing different variants of MSL2 (MSL2*) were calculated as a ratio of females to males in MSL2*/TM6,Tb (heterozygous) or MSL2*/MSL2* (homozygous) lines. At least 300 males and females were counted in each of three independent experiments.

Fly extract preparation

Twenty adult flies were homogenized with a pestle in 200 µl of 1×PBS containing 1% β-mercaptoethanol, 10 mM PMSF and 1:100 Calbiochem Complete Protease Inhibitor Cocktail VII. The suspension was sonicated three times for 5 s at 5 W. Then, 200 µl of 4×SDS-PAGE sample buffer was added and the mixture was incubated for 10 min at 100°C and centrifuged at 16,000 g for 10 min.

RNA isolation and quantitative analysis

Total RNA was isolated from 2- to 3-day-old adult males and females using the TRI reagent (Molecular Research Center) according to the manufacturer's instructions. RNA was treated with two units of Turbo DNase I (Ambion) for 30 min at 37°C to eliminate genomic DNA. The synthesis of cDNA was performed using 2 µg of RNA, 50 U of ArrayScript

reverse transcriptase (Ambion) and 1 µM of oligo(dT) as a primer. The amounts of specific cDNA fragments were quantified by real-time PCR with Taqman probes. At least three independent measurements were made for each RNA sample. Relative levels of mRNA expression were calculated in the linear amplification range by calibration to a standard genomic DNA curve to account for differences in primer efficiencies. Individual expression values were normalized with reference to *RpL32* mRNA.

The sequences of primers and oligonucleotides used in this work are given in Table S1.

Immunostaining of polytene chromosomes

Drosophila 3rd instar larvae were cultured at 18°C under standard conditions. Polytene chromosome staining was performed as described (Murawska and Brehm, 2012). The following primary antibodies were used: rabbit anti-MSL1 at 1:100 dilution, rabbit anti-MSL2 at 1:100 dilution, and monoclonal mouse anti-FLAG at 1:100 dilution. The secondary antibodies were Alexa Fluor 488 goat anti-mouse 1:2000 and Alexa Fluor 555 goat anti-rabbit 1:2000 (Invitrogen). The polytene chromosomes were co-stained with DAPI (AppliChem). Images were acquired on the Nikon Eclipse Ti fluorescence microscope using Nikon DS-Qi2 digital camera, processed with ImageJ 1.50c4 and Fiji bundle 2.0.0-rc-46. Three or four independent staining and four or five samples of polytene chromosomes were performed with each MSL2-expressing transgenic line.

Chromatin immunoprecipitation

Chromatin preparation was performed as described (Maksimenko et al., 2015; Zolotarev et al., 2017) with some modifications. Samples containing 10–20 µg of DNA equivalent in 1 ml of nuclear lysis buffer were incubated overnight, at 4°C, with rabbit antibodies against MSL1 (1:500), MSL2 (1:200) and CLAMP (1:200), or with nonspecific IgG purified from rabbit preimmune sera (control). Chromatin–antibody complexes were collected using blocked Protein A agarose at 4°C over 5 h. After several rounds of washing with one portion of lysis buffer, three portions of lysis buffer with 500 mM NaCl and one portion of TE buffer (10 mM Tris-HCl, pH 8; 1 mM EDTA), the DNA was eluted with elution buffer (50 mM Tris-HCl, pH 8.0; 1 mM EDTA, 1% SDS), the cross-links were reversed, and the precipitated DNA was extracted with phenol–chloroform. The enrichment of specific DNA fragments was analyzed by real-time PCR using a QuantStudio 12K Flex Cycler (Applied Biosystems). The primers used for PCR in ChIP experiments for genome fragments are shown in Table S1.

At least three independent biological replicates were made for each chromatin sample. The results of chromatin immunoprecipitation are presented as a percentage of input genomic DNA normalized to a positive control genomic site. Error bars show standard deviations of quadruplicate PCR measurements for three independent experiments. The *tubulin-γ37C* coding region (devoid of binding sites for the test proteins) were used as negative controls; Autosomal MSL1-binding region 26E3, MSL2-binding region 25A3 and CLAMP-binding region 39A1 were used as positive genomic controls.

Acknowledgements

We thank Farhod Hasanov and Aleksander Parshikov for fly injections, and Olga Kyrchanova for help with fly genetics. This study was performed using the equipment of the IGB RAS Core Facilities Centre, supported by the Ministry of Science and Education of the Russian Federation.

Competing interests

The authors declare no competing or financial interests.

Author contributions

Conceptualization: P.G., O.M.; Methodology: O.M.; Formal analysis: E.T., O.M.; Investigation: E.T., A.F., A.B., V.M., O.M.; Writing - original draft: P.G., O.M.; Writing - review & editing: E.N.L., P.G., O.M.; Visualization: E.T., A.F., A.B., V.M.; Supervision: P.G., O.M.; Funding acquisition: O.M.

Funding

This study was supported by the Russian Science Foundation (project no. 17-74-20155 to O.M.).

Supplementary information

Supplementary information available online at <http://dev.biologists.org/lookup/doi/10.1242/dev.179663.supplemental>

References

- Albig, C., Tikhonova, E., Krause, S., Maksimenko, O., Regnard, C. and Becker, P. B. (2019). Factor cooperation for chromosome discrimination in *Drosophila*. *Nucleic Acids Res.* **47**, 1706-1724. doi:10.1093/nar/gky1238
- Alekseyenko, A. A., Peng, S., Larschan, E., Gorchakov, A. A., Lee, O.-K., Kharchenko, P., McGrath, S. D., Wang, C. I., Mardis, E. R., Park, P. J. et al. (2008). A sequence motif within chromatin entry sites directs MSL establishment on the *Drosophila* X chromosome. *Cell* **134**, 599-609. doi:10.1016/j.cell.2008.06.033
- Bai, X., Alekseyenko, A. A. and Kuroda, M. I. (2004). Sequence-specific targeting of MSL complex regulates transcription of the roX RNA genes. *EMBO J.* **23**, 2853-2861. doi:10.1038/sj.emboj.7600299
- Bischof, J., Maeda, R. K., Hediger, M., Karch, F. and Basler, K. (2007). An optimized transgenesis system for *Drosophila* using germ-line-specific phiC31 integrases. *Proc. Natl. Acad. Sci. USA* **104**, 3312-3317. doi:10.1073/pnas.0611511104
- Fauth, T., Müller-Planitz, F., König, C., Straub, T. and Becker, P. B. (2010). The DNA binding CXC domain of MSL2 is required for faithful targeting the Dosage Compensation Complex to the X chromosome. *Nucleic Acids Res.* **38**, 3209-3221. doi:10.1093/nar/gkq026
- Hallacli, E., Lipp, M., Georgiev, P., Spielman, C., Cusack, S., Akhtar, A. and Kadlec, J. (2012). Msl1-mediated dimerization of the dosage compensation complex is essential for male X-chromosome regulation in *Drosophila*. *Mol. Cell* **48**, 587-600. doi:10.1016/j.molcel.2012.09.014
- Ilik, I. A., Maticzka, D., Georgiev, P., Gutierrez, N. M., Backofen, R. and Akhtar, A. (2017). A mutually exclusive stem-loop arrangement in roX2 RNA is essential for X-chromosome regulation in *Drosophila*. *Genes Dev.* **31**, 1973-1987. doi:10.1101/gad.304600.117
- Kadlec, J., Hallacli, E., Lipp, M., Holz, H., Sanchez-Weatherby, J., Cusack, S. and Akhtar, A. (2011). Structural basis for MOF and MSL3 recruitment into the dosage compensation complex by MSL1. *Nat. Struct. Mol. Biol.* **18**, 142-149. doi:10.1038/nsmb.1960
- Kelley, R. L., Wang, J., Bell, L. and Kuroda, M. I. (1997). Sex lethal controls dosage compensation in *Drosophila* by a non-splicing mechanism. *Nature* **387**, 195-199. doi:10.1038/387195a0
- Kuroda, M. I., Hilfiker, A. and Lucchesi, J. C. (2016). Dosage compensation in *Drosophila*-a model for the coordinate regulation of transcription. *Genetics* **204**, 435-450. doi:10.1534/genetics.115.185108
- Kuzu, G., Kaye, E. G., Chery, J., Siggers, T., Yang, L., Dobson, J. R., Boor, S., Bliss, J., Liu, W., Jogl, G. et al. (2016). Expansion of GA dinucleotide repeats increases the density of CLAMP binding sites on the X-chromosome to promote *Drosophila* dosage compensation. *PLoS Genet.* **12**, e1006120. doi:10.1371/journal.pgen.1006120
- Larschan, E., Soruco, M. M. L., Lee, O.-K., Peng, S., Bishop, E., Chery, J., Goebel, K., Feng, J., Park, P. J. and Kuroda, M. I. (2012). Identification of chromatin-associated regulators of MSL complex targeting in *Drosophila* dosage compensation. *PLoS Genet.* **8**, e1002830. doi:10.1371/journal.pgen.1002830
- Li, F., Parry, D. A. D. and Scott, M. J. (2005). The amino-terminal region of *Drosophila* MSL1 contains basic, glycine-rich, and leucine zipper-like motifs that promote X chromosome binding, self-association, and MSL2 binding, respectively. *Mol. Cell. Biol.* **25**, 8913-8924. doi:10.1128/MCB.25.20.8913-8924.2005
- Li, F., Schiemann, A. H. and Scott, M. J. (2008). Incorporation of the noncoding roX RNAs alters the chromatin-binding specificity of the *Drosophila* MSL1/MSL2 complex. *Mol. Cell. Biol.* **28**, 1252-1264. doi:10.1128/MCB.00910-07
- Lucchesi, J. C. (2018). Transcriptional modulation of entire chromosomes: dosage compensation. *J. Genet.* **97**, 357-364. doi:10.1007/s12041-018-0919-7
- Lyman, L. M., Copps, K., Rastelli, L., Kelley, R. L. and Kuroda, M. I. (1997). *Drosophila* male-specific lethal-2 protein: structure/function analysis and dependence on MSL-1 for chromosome association. *Genetics* **147**, 1743-1753.
- Maenner, S., Müller, M., Fröhlich, J., Langer, D. and Becker, P. B. (2013). ATP-dependent roX RNA remodeling by the helicase maleless enables specific association of MSL proteins. *Mol. Cell* **51**, 174-184. doi:10.1016/j.molcel.2013.06.011
- Maksimenko, O., Bartkuhn, M., Stakhov, V., Herold, M., Zolotarev, N., Jox, T., Buxa, M. K., Kirsch, R., Bonchuk, A., Fedotova, A. et al. (2015). Two new insulator proteins, Pita and ZIPIC, target CP190 to chromatin. *Genome Res.* **25**, 89-99. doi:10.1101/gr.174169.114
- Meller, V. H. and Rattner, B. P. (2002). The roX genes encode redundant male-specific lethal transcripts required for targeting of the MSL complex. *EMBO J.* **21**, 1084-1091. doi:10.1093/emboj/21.5.1084
- Meller, V. H., Wu, K. H., Roman, G., Kuroda, M. I. and Davis, R. L. (1997). roX1 RNA paints the X chromosome of male *Drosophila* and is regulated by the dosage compensation system. *Cell* **88**, 445-457. doi:10.1016/S0092-8674(00)81885-1
- Morra, R., Yokoyama, R., Ling, H. and Lucchesi, J. C. (2011). Role of the ATPase/helicase maleless (MLE) in the assembly, targeting, spreading and function of the male-specific lethal (MSL) complex of *Drosophila*. *Epigenetics Chromatin* **4**, 6. doi:10.1186/1756-8935-4-6
- Murawska, M. and Brehm, A. (2012). Immunostaining of *Drosophila* polytene chromosomes to investigate recruitment of chromatin-binding proteins. *Methods Mol. Biol.* **809**, 267-277. doi:10.1007/978-1-61779-376-9_18
- Quinn, J. J., Ilik, I. A., Qu, K., Georgiev, P., Chu, C., Akhtar, A. and Chang, H. Y. (2014). Revealing long noncoding RNA architecture and functions using domain-specific chromatin isolation by RNA purification. *Nat. Biotechnol.* **32**, 933-940. doi:10.1038/nbt.2943
- Rattner, B. P. and Meller, V. H. (2004). *Drosophila* male-specific lethal 2 protein controls sex-specific expression of the roX genes. *Genetics* **166**, 1825-1832. doi:10.1534/genetics.166.4.1825
- Samata, M. and Akhtar, A. (2018). Dosage compensation of the X chromosome: a complex epigenetic assignment involving chromatin regulators and long noncoding RNAs. *Annu. Rev. Biochem.* **87**, 323-350. doi:10.1146/annurev-biochem-062917-011816
- Scott, M. J., Pan, L. L., Cleland, S. B., Knox, A. L. and Heinrich, J. (2000). MSL1 plays a central role in assembly of the MSL complex, essential for dosage compensation in *Drosophila*. *EMBO J.* **19**, 144-155. doi:10.1093/emboj/19.1.144
- Soruco, M. M., Chery, J., Bishop, E. P., Siggers, T., Tolstorukov, M. Y., Leydon, A. R., Sugden, A. U., Goebel, K., Feng, J., Xia, P. et al. (2013). The CLAMP protein links the MSL complex to the X chromosome during *Drosophila* dosage compensation. *Genes Dev.* **27**, 1551-1556. doi:10.1101/gad.214585.113
- Straub, T., Grimaud, C., Gilfillan, G. D., Mitterweger, A. and Becker, P. B. (2008). The chromosomal high-affinity binding sites for the *Drosophila* dosage compensation complex. *PLoS Genet.* **4**, e1000302. doi:10.1371/journal.pgen.1000302
- Straub, T., Zabel, A., Gilfillan, G. D., Feller, C. and Becker, P. B. (2013). Different chromatin interfaces of the *Drosophila* dosage compensation complex revealed by high-shear ChIP-seq. *Genome Res.* **23**, 473-485. doi:10.1101/gr.146407.112
- Urban, J., Kuzu, G., Bowman, S., Scruggs, B., Henriques, T., Kingston, R., Adelman, K., Tolstorukov, M. and Larschan, E. (2017a). Enhanced chromatin accessibility of the dosage compensated *Drosophila* male X-chromosome requires the CLAMP zinc finger protein. *PLoS ONE* **12**, e0186855. doi:10.1371/journal.pone.0186855
- Urban, J. A., Doherty, C. A., Jordan, W. T., III, Bliss, J. E., Feng, J., Soruco, M. M., Rieder, L. E., Tsiarli, M. A. and Larschan, E. N. (2017b). The essential *Drosophila* CLAMP protein differentially regulates non-coding roX RNAs in male and females. *Chromosome Res.* **25**, 101-113. doi:10.1007/s10577-016-9541-9
- Villa, R., Schauer, T., Smialowski, P., Straub, T. and Becker, P. B. (2016). PionX sites mark the X chromosome for dosage compensation. *Nature* **537**, 244-248. doi:10.1038/nature19338
- Zheng, S., Villa, R., Wang, J., Feng, Y., Becker, P. B. and Ye, K. (2014). Structural basis of X chromosome DNA recognition by the MSL2 CXC domain during *Drosophila* dosage compensation. *Genes Dev.* **28**, 2652-2662. doi:10.1101/gad.250936.114
- Zhou, S., Yang, Y., Scott, M. J., Pannuti, A., Fehr, K. C., Eisen, A., Koonin, E. V., Fouts, D. L., Wrightsman, R., Manning, J. E. et al. (1995). Male-specific lethal 2, a dosage compensation gene of *Drosophila*, undergoes sex-specific regulation and encodes a protein with a RING finger and a metallothionein-like cysteine cluster. *EMBO J.* **14**, 2884-2895. doi:10.1002/j.1460-2075.1995.tb07288.x
- Zolotarev, N., Maksimenko, O., Kyrchanova, O., Sokolinskaya, E., Osadchii, I., Girardot, C., Bonchuk, A., Ciglar, L., Furlong, E. E. M. and Georgiev, P. (2017). Otpb is a new architectural/insulator protein required for ribosomal gene expression. *Nucleic Acids Res.* **45**, 12285-12300. doi:10.1093/nar/gkx840

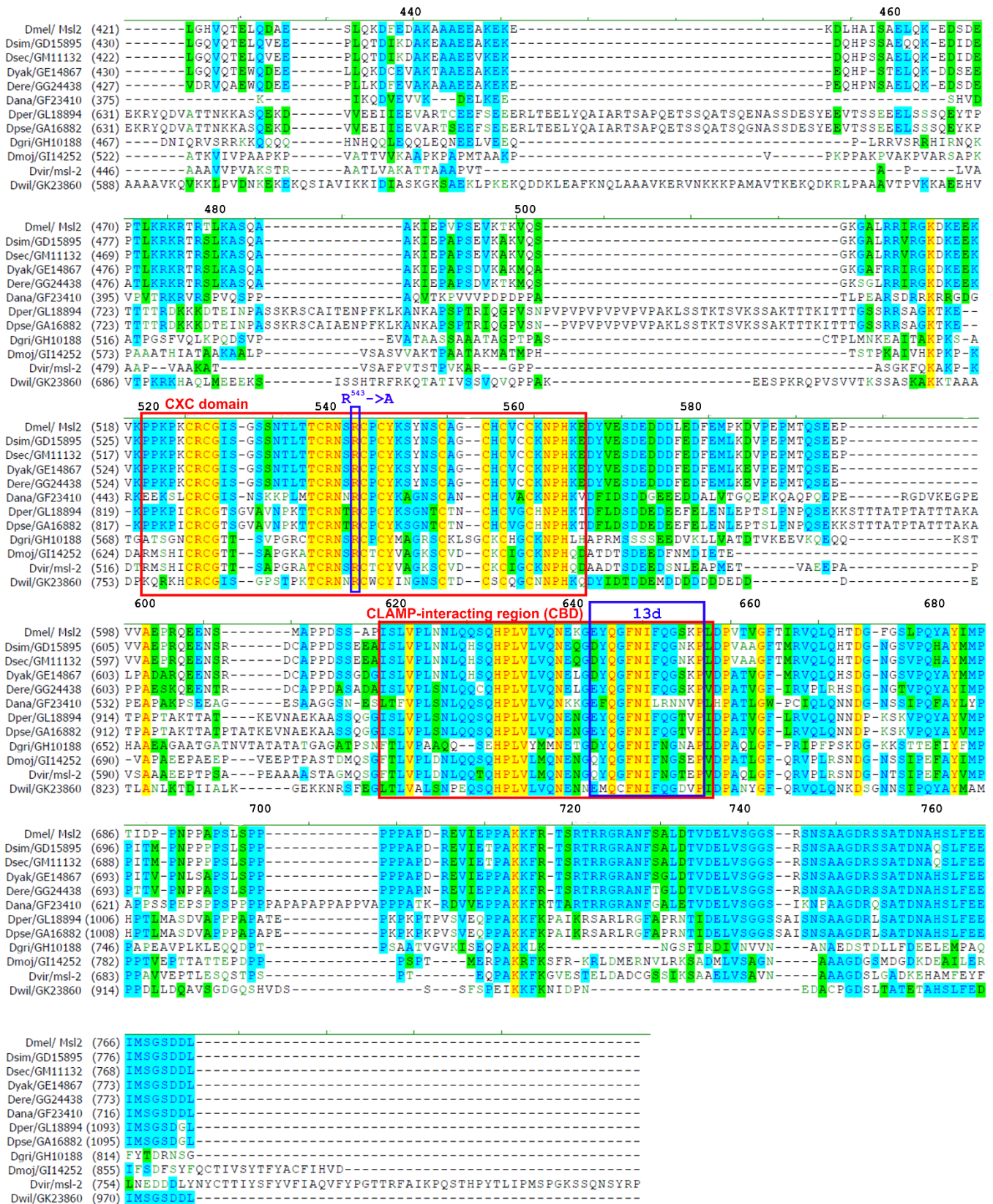


Figure S1. Alignment of MSL2 protein among Drosophilidae. Different regions are shown in the red frames. Also R543 amino acid residue and minimal 13 aa CLAMP-interacting region are marked in blue frames.

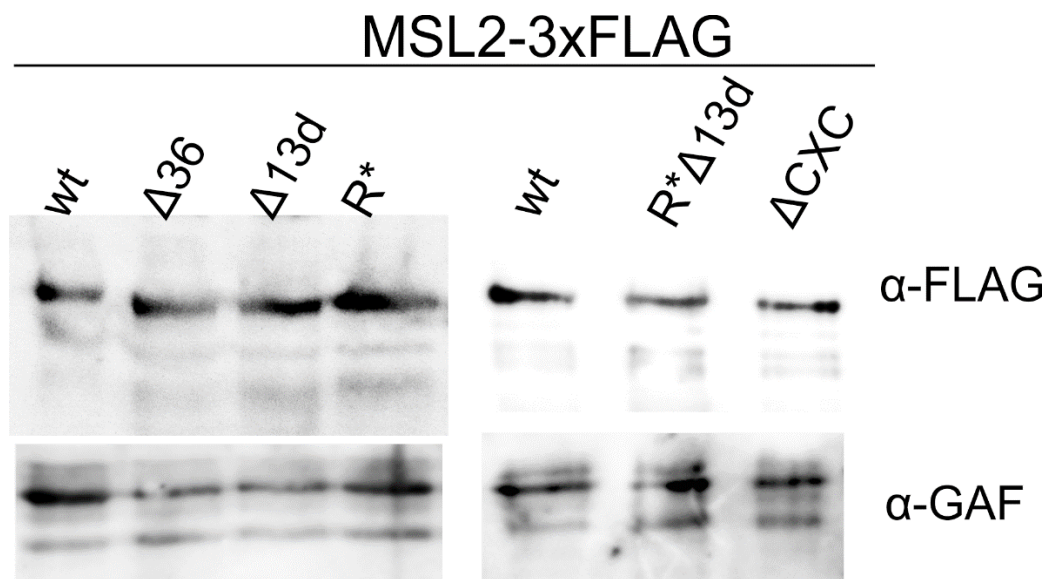


Figure S2.

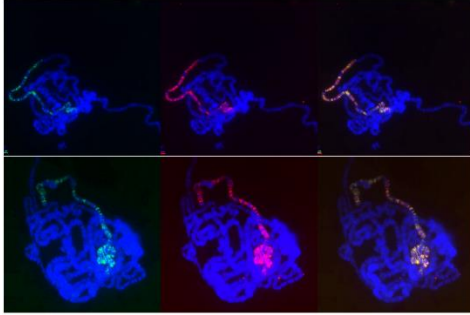
Western blotting of protein extracts prepared from adult flies expressing different variants of 3xFLAG-tagged MSL2 protein (wild-type (wt), deletion of 36 ($\Delta 36$) and 13 ($\Delta 13d$) aa from CLAMP-binding region, substitution of arginine at the 543 position by alanine (R*), simultaneous substitution of arginine at the 543 position by alanine and deletion of 13 aa from CLAMP-binding region (R* $\Delta 13d$), deletion of CXC domain (ΔCXC)).

Immunoblot analysis was performed with FLAG and GAF antibodies (internal control).

♂ *msl2²²⁷*

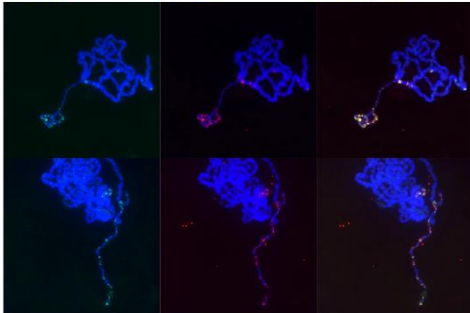
MSL2^{wt}-3xFLAG

FLAG MSL1 merged



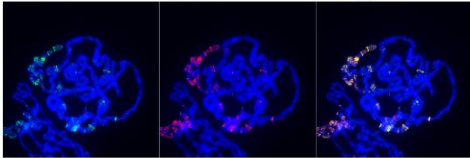
MSL2^{Δ13d}-3xFLAG

FLAG MSL1 merged



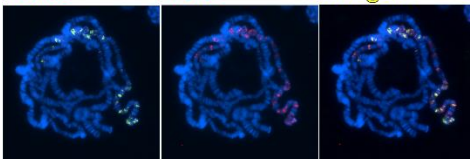
MSL2^{R*}-3xFLAG

FLAG MSL1 merged



MSL2^{ΔCXC}-3xFLAG

FLAG MSL1 merged



MSL2^{R*Δ13d}-3xFLAG

FLAG MSL1 merged

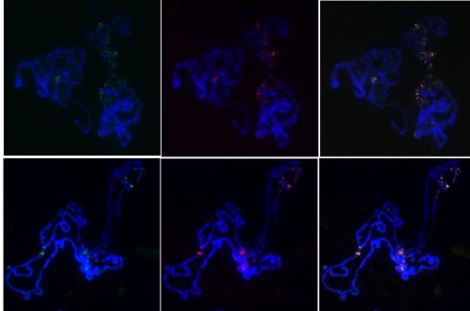
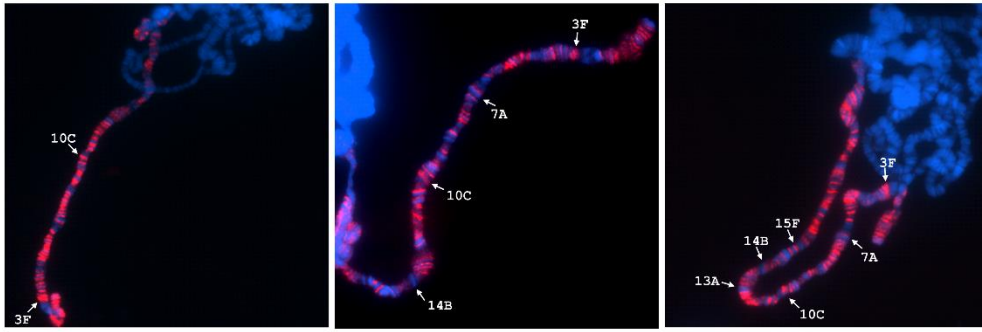


Figure S3. MSL1 and MSL2 localization on the polytene chromosomes from salivary glands of male 3rd instar larvae in the *msl2*-null (*msl2²²⁷*) background that express different FLAG-tagged variants of MSL2 protein: wild-type (wt), deletion of 13 aa from CLAMP-binding region ($\Delta 13d$), substitution of arginine at the 543 position by alanine (R*), deletion of CXC domain

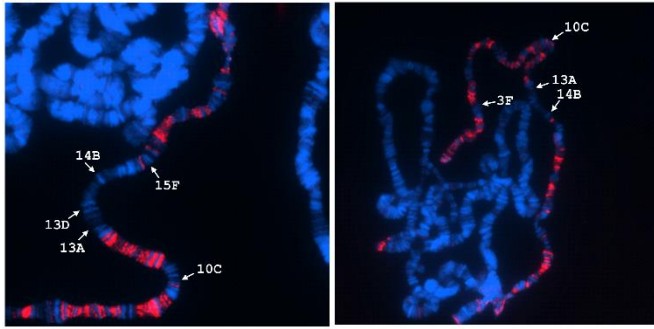
(Δ CXC), simultaneous substitution of arginine at the 543 position by alanine and deletion of 13 aa from CLAMP-binding region (R* Δ 13d). Panels show immunostaining of 3xFLAG-MSL2 protein with mouse anti-FLAG antibody (green) and MSL1 protein with corresponding rabbit antibody (red) on polytene chromosomes. DNA is stained with DAPI (blue).

♂ *msl2*²²⁷

MSL2^{wt}-3xFLAG

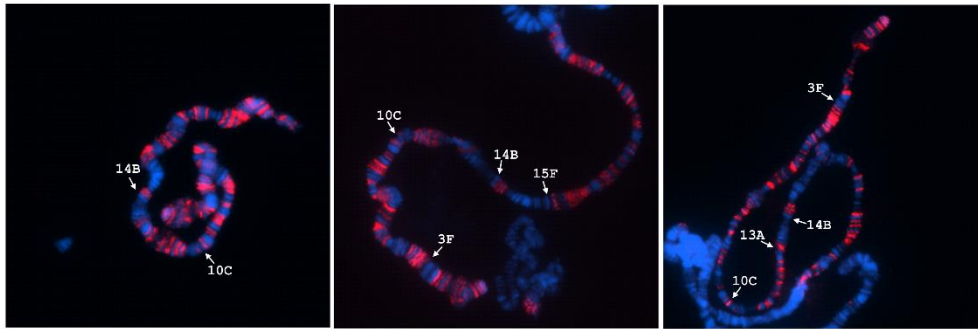


MSL2^{Δ13d}-3xFLAG

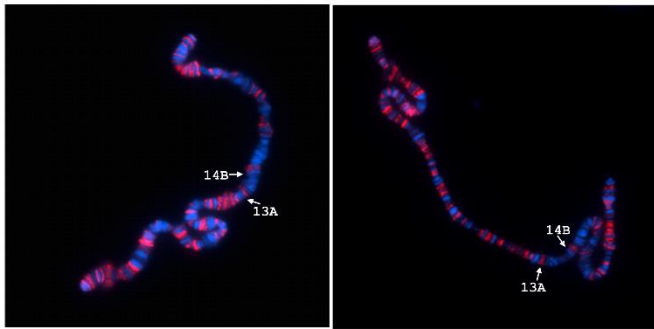


MSL2
DAPI

MSL2^{R+}-3xFLAG



MSL2^{ΔCXC}-3xFLAG



MSL2^{R+Δ13d}-3xFLAG

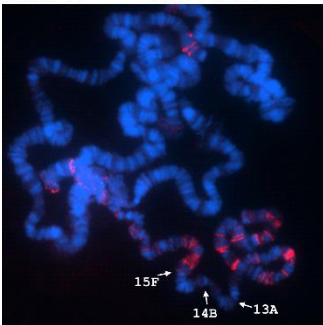


Figure S4. Comparing several sites of MSL complex binding at the high resolution cytological map on the polytene chromosomes from salivary glands of male 3rd instar larvae in the *msl2*-null (*msl2*²²⁷) background that expressed different FLAG-tagged variants of MSL2 protein: wild-

type (wt), deletion of 13 aa from CLAMP-binding region ($\Delta 13d$), substitution of arginine at the 543 position by alanine (R*), deletion of CXC domain (ΔCXC), simultaneous substitution of arginine at the 543 position by alanine and deletion of 13 aa from CLAMP-binding region (R* $\Delta 13d$). Panels show immunostaining of 3xFLAG-MSL2 protein with rabbit anti-MSL2 antibody (red) on polytene chromosomes. DNA is stained with DAPI (blue).

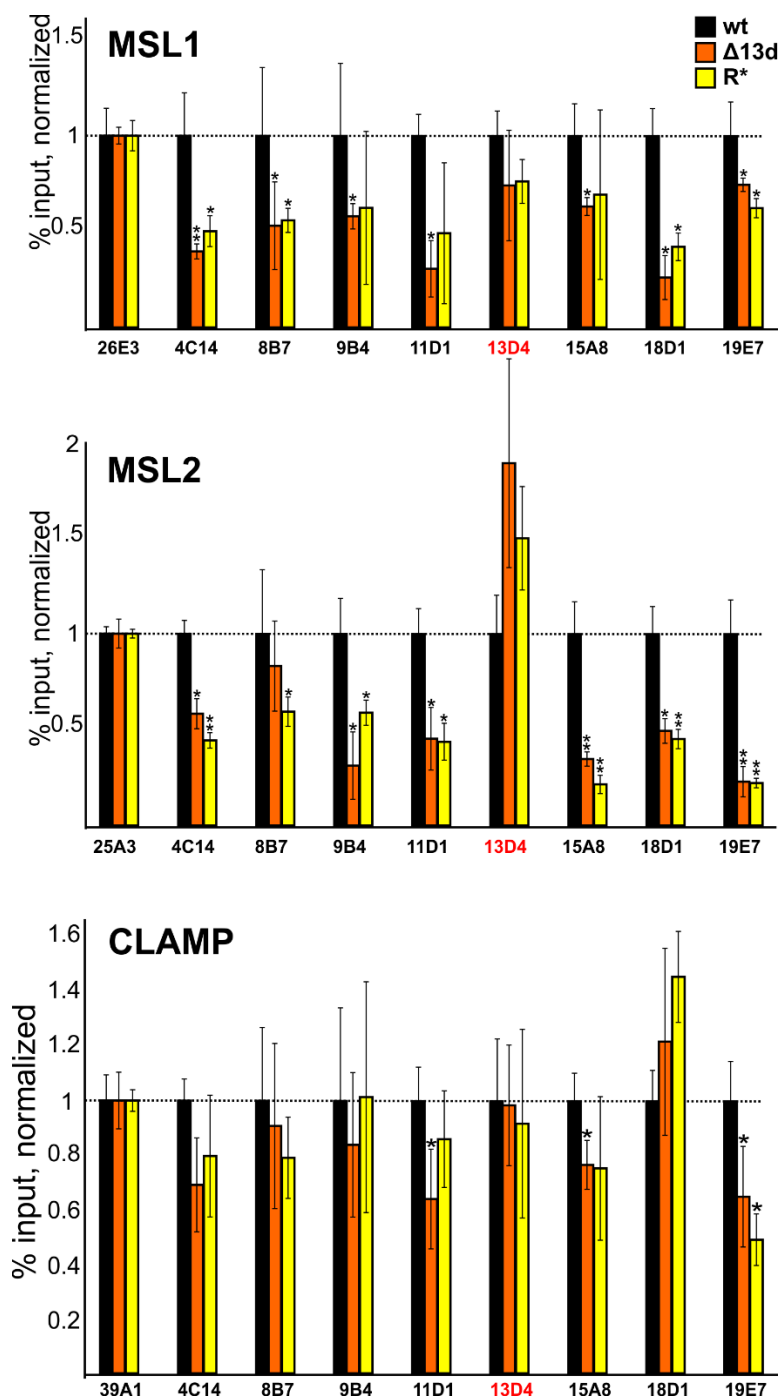


Figure S5. Comparing binding of MSL1, MSL2, and CLAMP at different CES and PionX (marked with red) regions in the MSL2-expressing males in the *msl2* ^{γ 227} background. Histograms show ChIP enrichments at the CES regions on chromatin isolated from male flies expressing different variants (wt, $\Delta 13d$, R*) of MSL2 protein. The results are presented as a percentage of input genomic DNA normalized to corresponding positive autosomal genome regions for MSL1(26E3) and MSL2 (25A3), and compared with binding levels in the flies with expressed wild type MSL2 protein (corresponding to the “1” on the scale). Error bars show standard deviations of quadruplicate PCR measurements for three independent experiments. Asterisks indicate significance levels: * $p < 0.05$, ** $p < 0.01$.

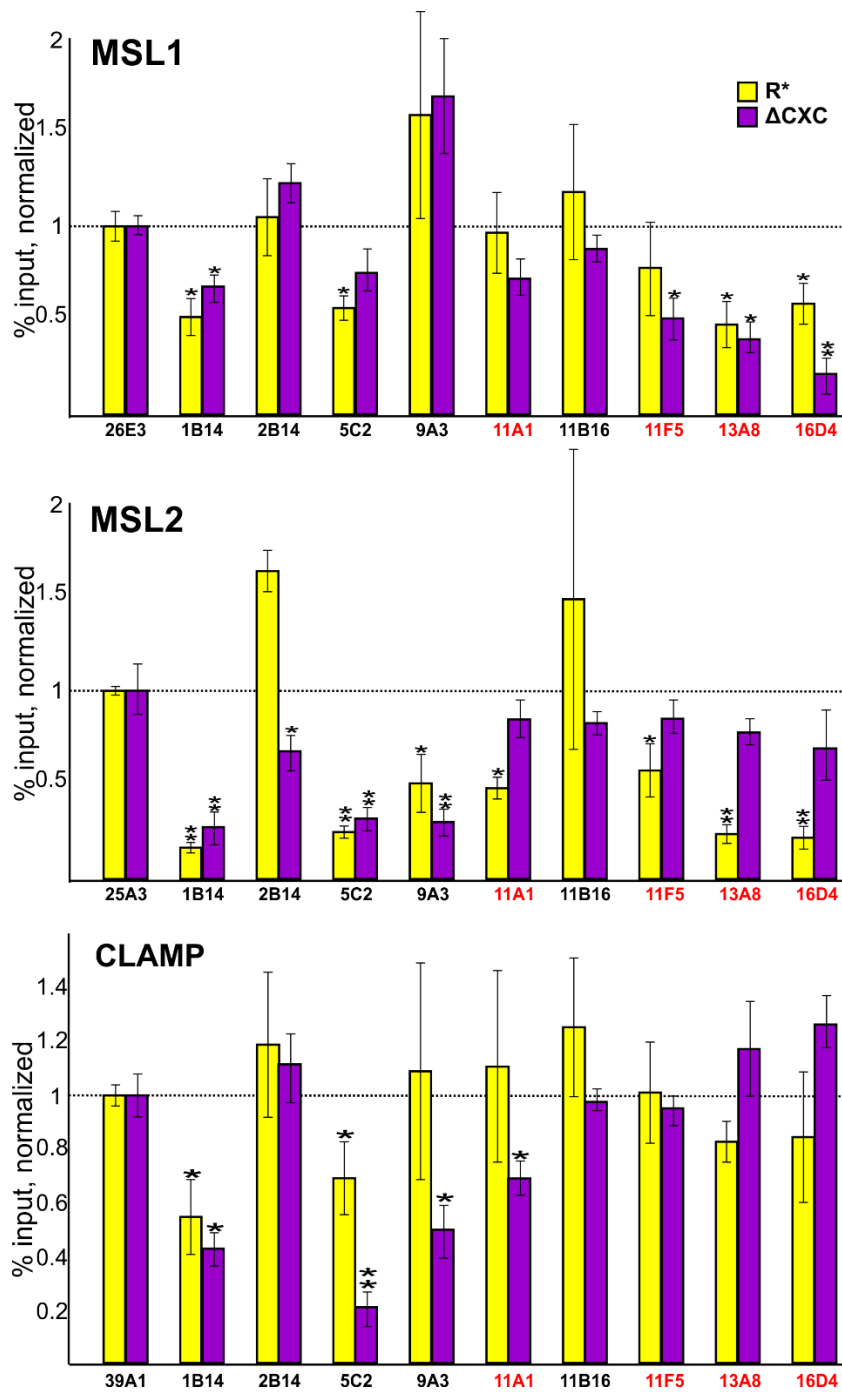


Figure S6. Comparing binding of MSL1, MSL2, and CLAMP at different CES and PionX (marked with red) regions in the MSL2-expressing flies in the *msl2*^{γ227} background. Histograms show comparison of ChIP enrichments at the CES regions on chromatin isolated from male flies expressed MSL2 protein with substitution of arginine at the 543 position by alanine (R*) and deletion of CXC domain (Δ CXC). The results are presented as a percentage of input genomic DNA normalized to corresponding positive autosomal genome regions for MSL1(26E3), MSL2 (25A3) and CLAMP (39A1), and compared with binding levels in the flies with expressed wild type MSL2 protein (corresponding to the “1” on the scale). Error bars show standard deviations of quadruplicate PCR measurements for three independent experiments. Asterisks indicate significance levels: * $p < 0.05$, ** $p < 0.01$.

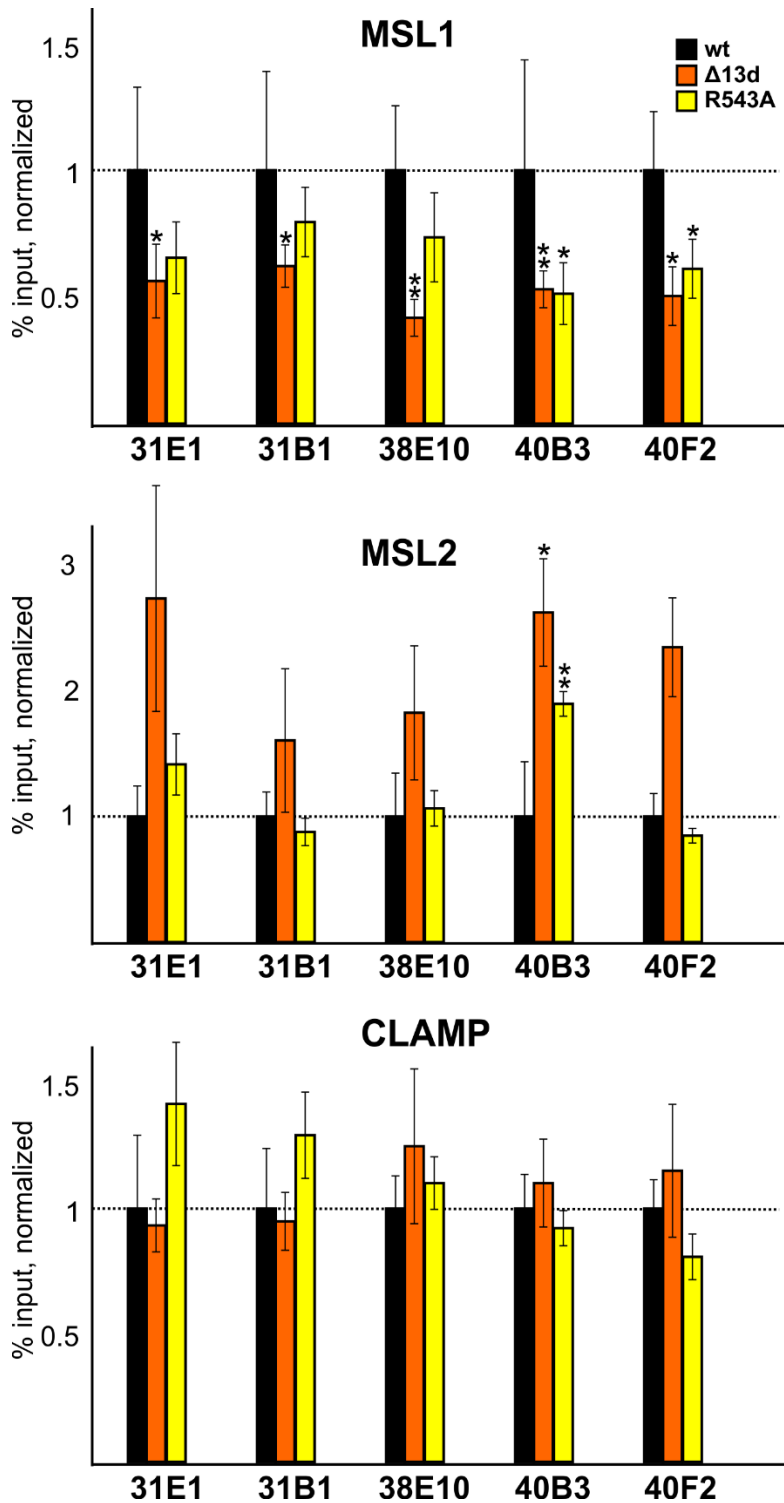


Figure S7. Comparing binding of MSL1, MSL2 and CLAMP at different autosomal genome regions in the MSL2-expressing flies in the *msl2^{γ227}* background. Histograms show ChIP enrichments at the CES regions on chromatin isolated from male flies expressing different variants (wt, Δ13d, R543A) of MSL2 protein. The results are presented as a percentage of input genomic DNA normalized to corresponding positive autosomal genome regions for MSL1(26E3), MSL2 (25A3), and compared with binding levels in the flies with expressed wild type MSL2 protein (corresponding to the “1” on the scale). Error bars show standard deviations of quadruplicate PCR measurements for three independent experiments. Asterisks indicate significance levels: * $p < 0.05$, ** $p < 0.01$.

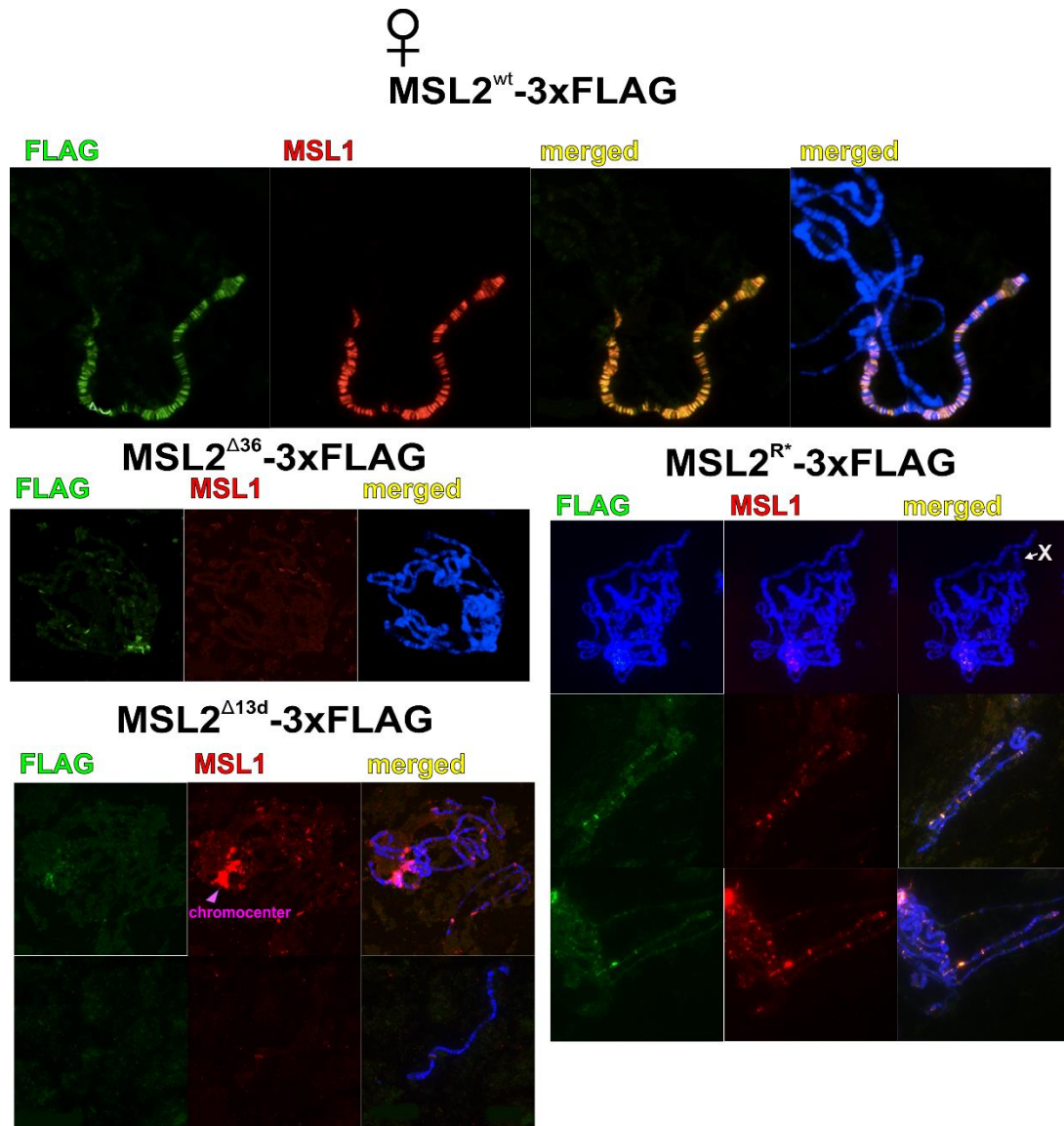


Figure S8. Distribution of MSL complex on the polytene chromosomes extracted from salivary glands of female 3rd instar larvae that express different FLAG-tagged variants of MSL2 protein: wild-type (wt), deletion of 36 ($\Delta 36$) and 13 ($\Delta 13d$) aa from CLAMP-binding region, substitution of arginine at the 543 position by alanine (R*). Panels show immunostaining of 3xFLAG-MSL2 protein with mouse anti-FLAG antibody (green) and MSL1 protein with corresponding rabbit antibody (red) on polytene chromosomes. DNA is stained with DAPI (blue).

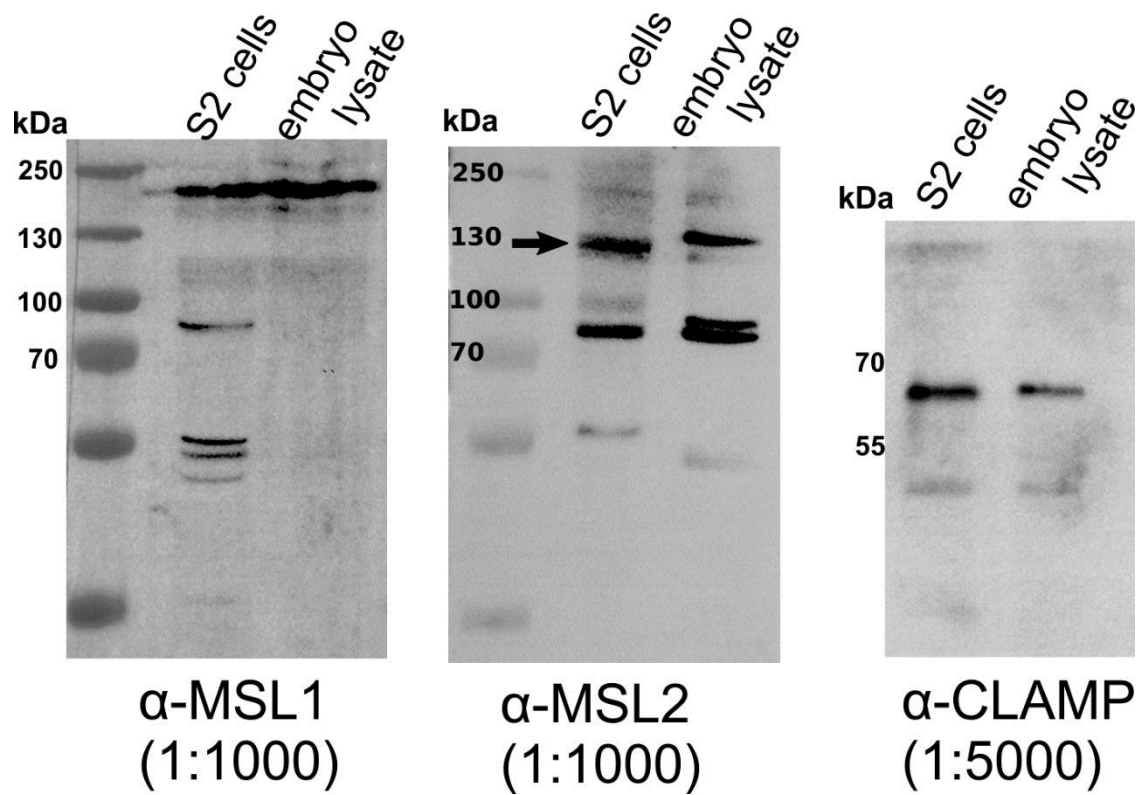


Figure S9. Immunoblot analysis of affinity-purified antibodies for MSL1, MSL2, CLAMP proteins.

Supplementary Table

Table S1. The list of used oligonucleotides.

Primers for cloning of <i>msl2</i> deletions			
Name	dir	rev	
<i>msl2</i> _full-sized	TTCGATATCATGGCCCAGACGGCATACTT	CCCGGGCAAGTCATCCGAGCCCGA	
<i>msl2</i> _d13	AAAGGCGAGGATCCGGTCACCGTTGG	GACCGGATCCTCGCCTTTCATTCT	
<i>msl2</i> _dB	CCACCGGCCCAACTTCTCGGCCCT	GAAGTTGGCGGCCGGTGGCTCGATGA	
<i>msl2</i> _dP	TATATAATGGCCAAGAAATTCAGGACC	TTTCTTGCCATTATATAAGCATACT	
Primers for RT-qPCR			
Name	dir	rev	Taqman probe
RoX1	CTTGTGCTTTCTCCTGAATGTG	TGTATTAGGCGGAGCTTCTTG	FAM-AGCCTATGAAATCCGGTCCAACCC-BHQ1
RoX2	TTCGAAACGTTCTCCGAAGC	AGTCGTACTCATCTCACTGTCC	FAM-AGCAAGAGTAACGATTTCGCGATAGTCG-BHQ1
RpL34	ACAACACACGCTCCAACA	GGGTGATACCCTTCAACTTCTC	FAM-TGGTAAACCAGACGACCACCGG-BHQ
Primers for ChIP analysis			
Genome region	dir	rev	
RoX1	AGGTCTGC AAGGTT CAGTTTAT	ATTCTTAAGGGTGGCGTCTTC	
RoX2	GGCTTAGAGAGAGATGGCAATAC	AGTTCTGGTACCCTGGA	
CES1B14	CAGGACAAGACTAGGACAAAAGG	GGTTTGGCGATTGAGGATTATTG	
CES2B14	CCCTCATATGCTTCTTCTGGTC	ACGTACGATCACGCACATATC	
CES4C14	ATTGGTATTCGGGCAAGGG	GAGCATATTTCTCTCGAGGATGG	
CES5C2	CAGAAATTCGAAGCGATCTCAAC	AATCGACTGCTAGGTTGGTAAA	
CES8B7	CAGCAGAACGCTCTTTGATTT	CCAACATTGCTTCACACAC	
CES9A3	TAATGCTGGATCTCGCTCAC	CTGATCGCCGGTCATAGAAA	
CES9B4	CGTGCCGCCTAACTATCTAAC	GGGATGAAAGAGAGAGCAAA	
CES11A1	GCCCAGAACTCCTTTAGTATG	TGATGCCACTGGATGAGTATG	
CES11B16	GGTGGTGGACATCTCGTTAAT	ACCAGCGAATATCGAGCATAAA	
CES11D1	AAGCCACTGATGCGTACAA	CAGAACGGCTGGCAAGATA	
CES11F5	TACAGTAGCTGAGAGCTGTACT	GTTTGGACTTGGCCTTTAC	
CES13A8	AATCTGAGCGAGATGGAAGAAC	GTGTCTAGTGGTTGGCTATGAC	
CES13D4	GCCGTGATTGTGGATCTCTT	CTCCAGACGTGCTGAATTGT	
CES15A8	CCAGGCTAAATAGTTCGC TACA	CGTAGTTGCATCTCGCTCTAAT	
CES16D4	CATCAACGACCTTGTACATTATC	GCACGAATCAGACAGAGAAGTA	
CES18D11	GCGCTTGCAATAGCTTCAATTA	GGAAATCCAAACAGTACAACCTCG	
CES19E7	GAGCGAGAGAGATTGCCAAATA	CGAATCGTGGAGTCTGAGAAAT	
26E3	CGTAACGGCACCCCTCAA	ACCGCACCGCACTACAAG	
25A3	GCTCCAGGAACCGATCTATTG	CTTGGCTTCCACTGAAGTTAGA	
39A1	CTCTGTTCACACAGCCATTTC	TACTCTTTCGGGCGGTATAA	
31E1	TGGATATGGCTTCTGGTTCATC	GGGCTGCATTCCGAGTTTA	
31B1	TTGTAAGGCGACTCGACTATTT	TGCTTTCGGCTGACTAATGA	
38E10	CGACACAAGTACCAGCTCTAAT	CGGCGAGGACTTACCATATTC	
40B3	GCAGAAGGGGAGAACTGTGAAATA	CTTCGCGGAGGGTTAATTGT	
40F2	CAGAACAACGCTCAGAGATAGA	GGGCTCTAAGAAATCCTACCAG	

Table S2. Cloning procedures

Pull down assay			
	dir	rev	Restriction sites
TRX-His-MSL2 [573-708]	ttggaattcatggaggactacgttg	agtgtcgacctattccctgtcaggagca	EcoRI Sall
TRX-His-CLAMP [1-153]	ctggaattcatggaagaccttacaa	aacgtcgacttccccgtctgtatgcat	EcoRI Sall
TRX-His-CLAMP [40-153]	ctggaattcatgaaaacggagcagcagc	aacgtcgacttccccgtctgtatgcat	EcoRI Sall
TRX-His-CLAMP [86-153]	-	-	HincII Sall
TRX-His-CLAMP [116-153]	-	-	MunI Sall
GST-CLAMP [1-196]	tacccgggatggaagaccttacaaaaac	aacgtcgacagacacaatctgtatctgg	SmaI Sall
GST-MSL2 [573-708]	ttggaattcatggaggactacgttg	agtgtcgacctattccctgtcaggagca	EcoRI Sall
GST-MSL2 [618-642]	-	-	BamHI RsaI
GST-MSL2 [618-655]	-	-	BamHI DpnI
GST-MSL2 [618-667]	-	-	BamHI PvuII
GST-MSL2 [618-687]	-	-	BamHI MunI
GST-MSL2 [651-708]	cagggatccaagccctgatccggtc	agtgtcgacctattccctgtcaggagca	BamHI Sall
GST-MSL2 [630-655]	ctcgatccatgcagcatccttgggt	gtggaattcctaatacaaggggcttg	BamHI EcoRI
GST-MSL2 [641-655]	-	gtggaattcctaatacaaggggcttg	BamHI EcoRI
Fly constructs			
pSK msl2-Fx3 full	ttcgatatcatggcccagacggcactt	tctccgggcaagtcacccagcccga	EcoRV SmaI
pSK msl2-Fx3 Δ36	accgatatcatggaggcatggatctg	tggactagttaggcttatggggcagaa	EcoRV SpeI
	ctcactagtcttgatccggcaccgt	tctccgggcaagtcacccagcccga	SpeI SmaI
pSK msl2-Fx3 Δ13d	ttcgatatcatggcccagacggcactt	gaccggatcctgcctttctcattct	EcoRV SmaI
	aaaggcgaggatccggcaccgttgg	tctccgggcaagtcacccagcccga	
pSK msl2-Fx3 R543A	atcgaattccgcctgtcctt	tctccgggcaagtcacccagcccga	EcoRI SmaI
pSK msl2-Fx3 ΔCXC	ttcgatatcatggcccagacggcactt	cggattcttctcggcttcggaggct	EcoRV SmaI
	aagccgaagaagaatccgcacaagga	cccgggcaagtcacccagcccga	
pSK msl2-Fx3 R543A ΔCXC	atcgaattccgcctgtcctt	tctccgggcaagtcacccagcccga	EcoRI SmaI
yil Ubi msl2-Fx3 full attB	-	-	EcoRV NotI
yil Ubi msl2-Fx3 Δ36 attB	-	-	EcoRV NotI
yil Ubi msl2-Fx3 Δ13d attB	-	-	EcoRV NotI
yil Ubi msl2-Fx3 R543A attB	-	-	EcoRV NotI
yil Ubi msl2-Fx3 ΔCXC attB	-	-	EcoRV NotI
yil Ubi msl2-Fx3 R543A ΔCXC attB	-	-	EcoRV NotI